Environmental and
Biogeochemical Processes

https://doi.org/10.48130/ebp-0025-0018

Original Research

Open Access

Bioextraction of residual phosphorus from phosphogypsum by phosphate-solubilizing fungus *Aspergillus niger*

Zhenyu Chao[1#], Haoxuan Li[1#], Jiakai Ji[1#], Xin Sun[1], Yuhang Sun[1], Meiyu Xu[1], Ying Wang[1], Da Tian[2], Haoming Chen[3], Dan Yu[4] and Zhen Li[1,5,6*]

Received: 12 September 2025

Revised: 4 December 2025

Accepted: 17 December 2025

Published online: 19 January 2026

Abstract

Phosphogypsum (PG) is a typical solid waste formed during wet-process phosphoric acid production, and it retains a significant amount of residual phosphorus (P). Bioextraction of phosphorus (BEP) applies microorganisms to dissolve P from phosphate minerals. This study aimed to evaluate the influence of gypsum ($CaSO_4$) on the BEP efficiency of PG by *Aspergillus niger*. After 6 d incubation with the addition of HPG (high dose of PG, 1.0 g), the biomass and respiration of *A. niger* reached 0.85 g and 8,937 μg C/kg/h, respectively. Meanwhile, the BEP efficiency of *A. niger* reached ~40% after 15 d of incubation, compared with ~10% in the treatment without the fungus. Given the amount consumed by *A. niger*, the efficiency should be significantly higher. Moreover, nanoscale secondary ion mass spectrometry (NanoSIMS) imaging showed that P was absorbed by *A. niger* cells to meet their nutritional requirements. Simulation from Geochemist's® Workbench (GWB) revealed that PO_4^{3-} tended to combine with Ca^{2+} and mineralize into hydroxylapatite as pH increased. However, oxalic acid secreted by *A. niger* would combine with the abundant Ca^{2+} in PG to produce CaC_2O_4, thereby reducing the fixation of P by free Ca^{2+}. Furthermore, the SO_4^{2-} from PG participated in the biosynthesis of sulfur-containing amino acids within the fungal cells. This study revealed the potential of BEP by *A. niger* for the treatment of solid waste PG.

Keywords: Bioextraction, Phosphorus, Phosphogypsum, Gypsum, *Aspergillus niger*

Highlights

- Oxalic acid secreted by *A. niger* would preferentially combine with Ca^{2+} in PG to produce CaC_2O_4.
- The formation of CaC_2O_4 reduced the reabsorption of P by Ca^{2+}.
- SO_4^{2-} from PG participated in the biosynthesis of sulfur-containing amino acids within the *A. niger* cells.
- High bioactivity of *A. niger* promoted further bioextraction of P from PG.
- The BESP efficiency is over 40% after 15 d of incubation.

Authors contributed equally: Zhenyu Chao; Haoxuan Li and Jiakai Ji

* Correspondence: Zhen Li (lizhen@njau.edu.cn)

Full list of author information is available at the end of the article.

https://doi.org/10.48130/ebp-0025-0018

Graphical abstract

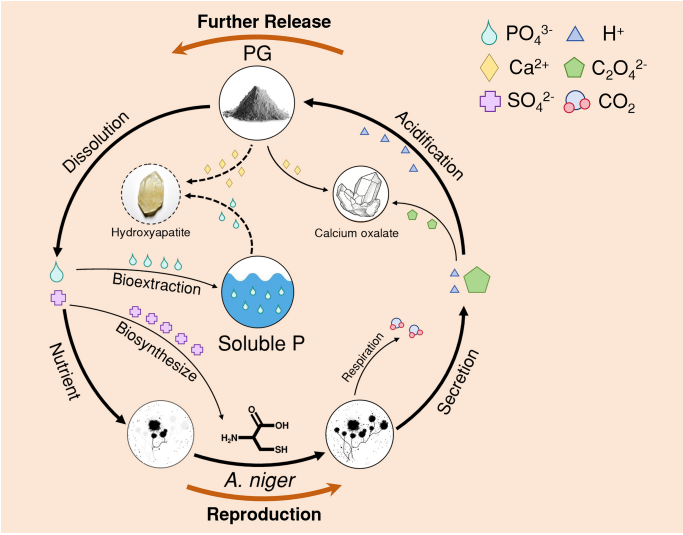

Introduction

Phosphogypsum (PG) is a solid waste residue generated from the treatment of phosphate rock with sulfuric acid during phosphoric acid production. Its primary component is gypsum ($CaSO_4{\cdot}2H_2O$). The fluorides, radionuclides, and heavy metals present in PG pose a risk of environmental pollution[1]. Now, PG is causing environmental risk globally. Approximately 300 million tons of PG are produced worldwide annually[2,3], of which 58% are dumped[4]. In addition, only 14% PG are currently reused. It is worth noting that over 3 billion tons of additional PG stacks have been built globally, which will cause resource waste[5,6]. PG contains approximately 1% P (mainly as the form of insoluble phosphate)[6–9]. Extraction of residual P can mitigate potential nonpoint-source pollution from the PG yard[10]. Meanwhile, it facilitates the utilization of residual P for agricultural purposes[11,12].

Bioextraction refers to the process of dissolving, recovering, or extracting valuable substances from raw materials by using organisms (primarily microorganisms, such as bacteria and fungi) or their metabolic products (such as organic acids and enzymes)[13]. Bioextraction aims to achieve optimal energy utilization through biotechnology[13,14]. This technology is considered as more environmentally friendly than chemical technology[15]. Bioextraction of sulfur and iron from waterlogged archeological wood by *Thiobacillus denitrificans* has been successfully performed. Bioextraction showed higher Fe extraction efficiency (65.1%) than chemical extraction (6.6%) of archaeological oak wood[16]. Similarly, iron-oxidizing bacteria and sulfur-oxidizing bacteria have been effectively employed in microbial-mediated copper bioextraction[17,18]. This strategy has been widely implemented for copper recovery from mining wastes and low-grade ores[19]. In the field of agriculture, traditional phosphate fertilizers pose environmental concerns, including eutrophication of adjacent water bodies due to low utilization rates, soil acidification resulting from the application of high-concentration phosphate fertilizers, and the depletion of phosphate rock resources driven by phosphate fertilizer production[20]. With respect to chemical phosphate fertilizers, fertilizers with the addition of functional microorganisms offer advantages such as pollution-free operation, high nutrient utilization efficiency, and alignment with the appeal of sustainable development[21].

Bioextraction of P (BEP) refers to the use of phosphate-solubilizing microorganisms (PSM) to convert P from an unavailable to an available form[22,23]. Phosphate-solubilizing fungi (PSF) secrete a wider range of organic acids (e.g., oxalic, citric, and gluconic acids) at higher production levels[24,25]. In addition, most PSF remain active under extreme drought or high-metal-concentration environments[26,27]. The excessive Ca^{2+} from PG can inhibit P dissolution by reducing its availability[28]. Organic acids secreted by microorganisms can substantially dissolve P[29–31], presumably by chelating Ca^{2+}. Meanwhile, the abundant SO_4^{2-} from PG serves as an S source, providing the S element for biosynthesis within PSM cells[32]. The BEP approach is cost-effective and sustainable[33–36].

Aspergillus niger (*A. niger*) is one of the highly efficient PSF[37,38]. It is a filamentous fungus whose hyphae can enter gaps between mineral particles to facilitate nutrient uptake[39]. *A. niger* itself requires P for the synthesis of essential biomolecules such as ATP and cell wall phospholipids[40]. *A. niger* mainly secretes oxalic acid and citric acid to dissolve insoluble phosphate[41,42]. The secretion abundance of oxalic acid and citric acid depends on the bioactivity of *A. niger* during incubation, which determines the efficiency of BEP[37,43].

This study aimed to evaluate the influence of gypsum on the BEP efficiency of PG by *A. niger*. The secondary minerals formed during incubation, the morphology of the fungal-mineral interaction, and the elemental distribution within fungal structures were studied.

Materials and methods

Preparation of PG and *A. niger*

The PG used in this experiment was collected from Fuquan City, Guizhou Province, China. PG was analyzed using a wavelength-dispersive X-ray fluorescence spectrometer (XRF).

A. niger (Accession No. M 2023240) was obtained from the China Center for Type Culture Collection (CCTCC). The information on *A. niger* in this experiment can be found in our previous study[44]. Before inoculation, the fungal spore suspension was thawed at 28 °C. The activation of *A. niger* was performed using Potato Dextrose Agar (PDA) medium.

A. niger incubation

The modified Pikovskaya Inorganic Phosphorus (PVK) medium employed in this study was formulated without any P source, while retaining the addition of 10.0 g dextrose, 0.03 g $FeSO_4·7H_2O$, 0.03 g $MgSO_4·7H_2O$, 0.3 g NaCl, 0.3 g KCl, 0.5 g $(NH_4)_2SO_4$, 0.03 g $MnSO_4·7H_2O$, and 1,000 mL ultrapure water[45].

For strain activation, *A. niger* spores were inoculated onto Potato Dextrose Agar (PDA) medium on a clean bench. The spore concentration was formed by expanding incubation at 28 °C for 6 d. Then, the medium surface was washed with sterile water on a clean bench, and the spores were carefully scraped off with a sterile inoculation ring to obtain a spore suspension. Finally, three layers of sterile gauze were used to filter the spore suspensions to remove broken mycelial fragments. Spore concentration was calculated with a blood cell counting plate, and the spore suspension was diluted to 10^7 cfu/mL with 0.85% sterile saline. For the incubation, serum bottles (150 mL) were filled with 50 mL of modified PVK medium. One mL of *A. niger* spore suspension was inoculated into a medium bottle with different P levels. Five experimental treatments were established, i.e., Control (0.25 g $Ca_3(PO_4)_2$ as P source), PFree (no P source), LPG (0.1 g PG as P source), MPG (0.5 g PG as P source), and HPG (1.0 g PG as P source). Each treatment was performed in triplicate.

A parallel experiment was set to investigate the BEP efficiency for *A. niger*. The incubation periods were set at 6, 10, and 15 d, respectively. For these three incubation periods, six treatments were set up, i.e., 6dPG, 6dPG + ANG, 10dPG, 10dPG + ANG, 15dPG, 15dPG + ANG, respectively (ANG represents the treatment in which was inoculated *A. niger*). Each treatment consisted of 50 mL of modified PVK medium and 1.0 g PG. The incubation conditions were identical to those in the above experiment. Each treatment was also performed in triplicate.

Sample preparation and chemical property analysis

After 6 d incubation, the serum bottles were filled with high-purity nitrogen gas (for 5 min) using a nitrogen evaporator (JH-NK200-1B). Then, the serum bottle was capped with a sealed stopper, and *A. niger* was incubated again for 0.5 h (28 °C, 180 rpm). Finally, after mixing the gas in the serum bottle with a syringe, 10 mL of the mixed gas was extracted for testing CO_2 emissions. In addition, the medium was filtered by using a 0.22-μm polyethersulfone (PES) membrane filter. Subsequently, pH values, total organic carbon (TOC), P concentrations, acid phosphatase activity (ACP), and oxalic acid concentration of the filtrate were measured.

After measuring the P concentrations, P extraction efficiencies were calculated according to the following formula:

$$\eta_P = \frac{C_R}{C_T} \times 100\%$$

where, η_P refers to the efficiency of BEP from the corresponding treatment; the C_R (mg/L) refers to the P concentration obtained by the ICP-OES test in the filtrate of the corresponding treatment; the C_T refers to the total P concentration of the corresponding treatment, which is the P concentration obtained by assuming that all P in the system is dissolved.

The solid phase obtained after filtration was dried in an oven at 65 °C, then weighed to determine the biomass of *A. niger*. After drying, the solid phase was determined by attenuated total reflection infrared spectroscopy (ATR-IR). Meanwhile, another round of the same incubation experiment was performed. The filtered solid phase was placed in a 2.5% glutaraldehyde solution for 12 h (25 °C). Then, a portion of the solid phase from the HPG treatment was embedded in resin and sectioned into 200 nm-thick slices for nanoscale secondary ion mass spectrometry (NanoSIMS) analysis. The remaining solid phase was dried in a vacuum freeze-dryer (Genscience Instrument Pro-4055, Nanjing, China). After drying, it was characterized by scanning electron microscopy-energy dispersive spectroscopy (SEM-EDS).

GWB modeling and data analyses

The Geochemist's® Workbench (GWB Version 12, USA) was applied to simulate the mineralization of Fe and the formation of CaC_2O_4[45]. The concentrations of HPO_4^{2-} and PO_4^{3-} were based on ICP-OES data.

Instrumentation

PG was analyzed by XRF (Thermo Fisher ARL Perform' X 4200). The effective diameter of the XRF analysis was 25 mm. CO_2 was measured by gas chromatography (GC) (Agilent 7890). The pH values of the filtrate were measured using a Mettler pH meter (Pro-ISM-IP67). The TOC of the filtrate was measured using a total organic carbon and nitrogen analyzer (Multi N/C3100). Concentrations of P were measured by ICP-OES (Optima 8000). Acid phosphatase (ACP) activity of the filtrate was measured with an acid phosphatase kit (Cominbio, Suzhou, China).

Concentrations of oxalic acid were measured by HPLC (Agilent 1200). The chromatographic column was SB-Aq (4.6 mm × 250 mm). The mobile phase consisted of 0.25% KH_2PO_4 buffer (pH 2.80) and methanol; the volume ratio was 99:1, the flow rate was 1 mL/min, the sample size was 20 μL, the column temperature was 30 °C, and the detection wavelength was 210 nm.

The infrared spectra were acquired using a Nicolet iS5 FTIR spectrometer (ThermoFisher Scientific Inc.). Data collection was performed using OMNIC software (Thermo Fisher Scientific Inc., Madison, USA) with the following parameters: spectral range of 500–2,000 cm^{-1}, 16 cumulative scans, and 4 cm^{-1} spectral resolution for each sample.

Elemental mapping was conducted using a NanoSIMS 50 analytical system (Cameca, Courbevoie, France). The hyphal pellets of *A. niger* were sectioned into semi-thin slices of 200 nm. Then, they were mounted on 10 mm-diameter silicon wafers. The microbial section specimens were continuously bombarded with a cesium ion (Cs^+) beam, inducing sputtering of secondary ions from the surface layers. After energy-based sorting in the electrostatic sector, these liberated ions were separated in a mass spectrometer based on their charge-to-mass ratios. The imaging protocol employed a dwell time of 1–3 ms/pixel and an image resolution of 512 × 512 pixels. Finally, the spatial mass distribution maps of $^{12}C^{14}N^-$ (characterizing nitrogen), $^{31}P^-$ and $^{32}S^-$ were produced.

SEM imaging was conducted using a Carl Zeiss Supra 55 system operated at 5–15 kV accelerating voltage. Before imaging, all samples were gold-sputtered for 5 min to minimize surface charging and enhance image quality. The semi-quantitative analysis was performed using an Oxford Aztec X-Max 150 energy-dispersive spectrometer (EDS) with a collection time of 90 s.

Results

TOC and biomass of *A. niger* - PG system

The TOC in Control treatment was 1.74 g/L (Fig. 1a). In contrast, the PFree treatment showed a significantly higher TOC concentration of 4.11 g/L (Fig. 1a). The addition of PG at a low level (LPG treatment) resulted in a lower concentration of 2.96 g/L, which was still higher than that of Control treatment (Fig. 1a). Moreover, the TOC concentrations of the MPG and HPG treatments were significantly

https://doi.org/10.48130/ebp-0025-0018

lower than that of Control treatment, being 0.38 and 0.36 g/L, respectively (Fig. 1a).

In the Control treatment, biomass was 0.30 g. The biomass of PFree treatment was as low as 0.05 g (Fig. 1a). In the LPG treatment, biomass was 0.13 g, which was significantly less than that of the Control treatment (Fig. 1a). In the MPG treatment, biomass increased to 0.43 g (Fig. 1a). In the HPG treatment, the biomass reached 0.85 g (Fig. 1a). Moreover, the biomass of *A. niger* increased with the reduction of TOC concentration, which showed a significant negative correlation (Fig. 1b).

Bioactivity of *A. niger*

The CO_2 emission rate of the Control treatment was 4,710 μg C/kg/h (Fig. 1c). In contrast, the respiration intensity of PFree treatment was the lowest, i.e., 470 μg C/kg/h (Fig. 1c). In the LPG treatment, the respiration intensity was 7,750 μg C/kg/h, which was significantly more than the Control treatment (Fig. 1c). In the MPG treatment, the respiration intensity was 4,273 μg C/kg/h, which showed no significant difference from Control treatment. In the HPG treatment, the respiration intensity reached 8,937 μg C/kg/h (Fig. 1c). The respiration

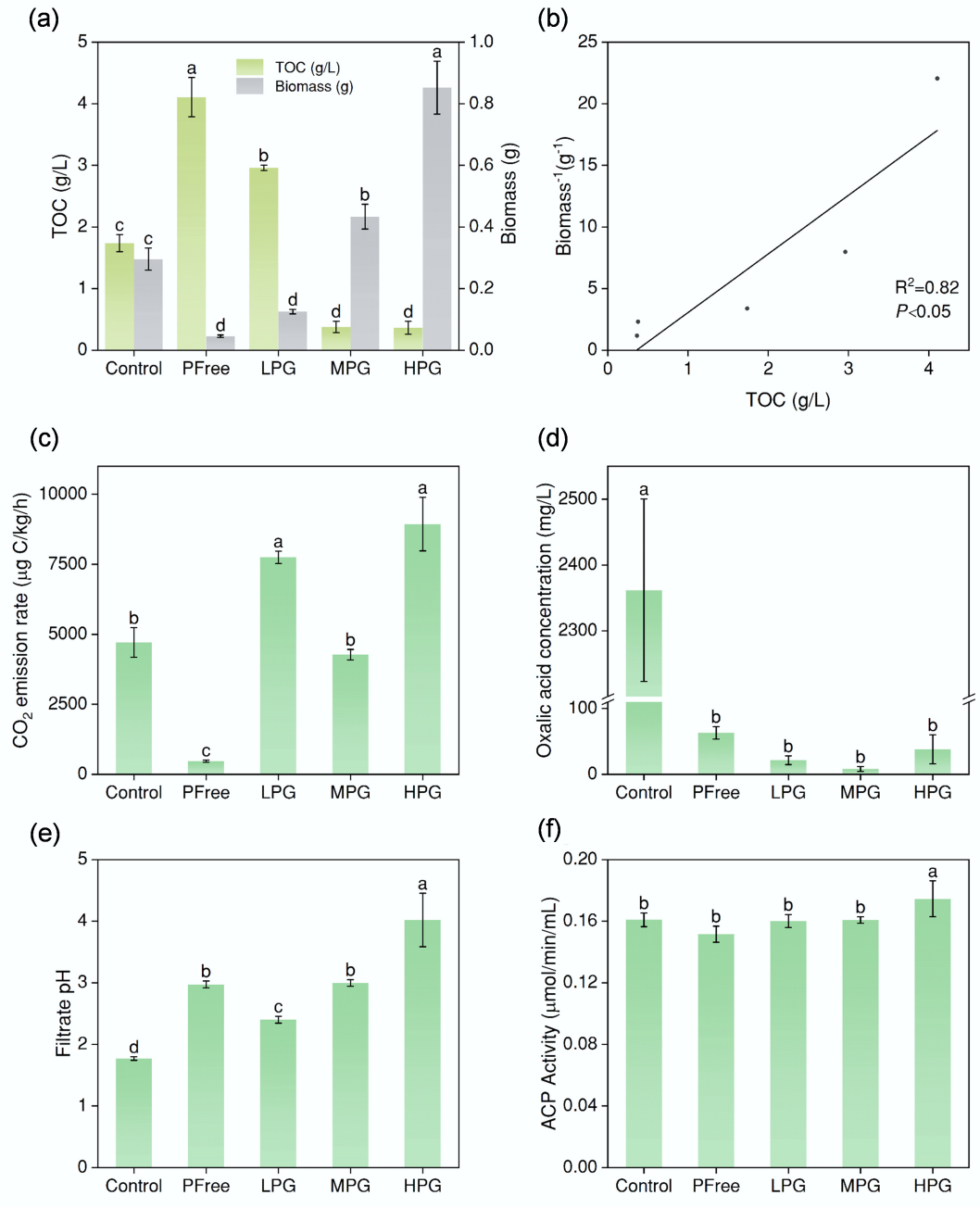

Fig. 1 Incubation effect of *A. niger*. (**a**) Biomass, and TOC content of filtrate after six days of incubation under different treatments. (**b**) The correlation between TOC values and the reciprocal of biomass. (**c**) CO_2 emission rates of the system. (**d**) Concentrations of oxalic acid secreted by *A. niger*. (**e**) pH values of the filtrate after incubation for six days. (**f**) acid phosphatase activity of filtrate after incubation for six days. (The lowercase letter labels in the figure indicate significant differences among different treatments. If two treatments contained the same lowercase letter, there was no significant difference between them; otherwise, there was a significant difference).

intensity of the above *A. niger* treated with P source was significantly stronger than that of PFree treatment (Fig. 1c).

The oxalic acid concentration in the Control treatment was recorded as 2,362 mg/L (Fig. 1d). When no P source was added during incubation, the PFree treatment showed a significantly lower oxalic acid concentration of 63 mg/L (Fig. 1d), which indicated the limited oxalic acid secretion of *A. niger* under P restriction. The oxalic acid concentrations in LPG, MPG, and HPG treatments were 21, 8, and 38 mg/L, respectively (Fig. 1d). The solubility of $CaSO_4{\cdot}2H_2O$ in pure water (0.264 g/100 g water, room temperature) is approximately 100 times that of $Ca_3(PO_4)_2$ (0.0025 g/100 g water, room temperature, from ChemBK). Therefore, the incubation system of *A. niger* with PG resulted in the generation of more CaC_2O_4 compared with the system of *A. niger* with $Ca_3(PO_4)_2$. In the HPLC test, the filtrate did not contain CaC_2O_4, resulting in extremely low oxalic acid concentrations measured after treatment with PG added.

In the Control treatment, the pH value was 1.8 (Fig. 1e). The pH value in the PFree treatment was 3.0 (Fig. 1e). The pH value significantly increased from 2.4 in the LPG treatment to 3.0 in the MPG treatment, and then increased dramatically to 4.0 in the HPG treatment (Fig. 1e). The pH values from PG treatments were all higher than those in the Control treatment (Fig. 1e).

In HPG treatment, the acid phosphatase activity of the filtrate reached 0.17 μmol/min/mL, which was significantly higher than that of LPG and MPG treatments (Fig. 1f). There was no significant difference in acid phosphatase activity among other treatments except for HPG treatment (Fig. 1f).

BEP efficiency

The P content in PG was as low as 0.81% according to XRF results. In the Control treatment, the BEP efficiency from $Ca_3(PO_4)_2$ by *A. niger* was 42.78% (Fig. 2c). In LPG, MPG, and HPG treatments, the BEP efficiency from PG by *A. niger* decreased dramatically to 10% level (8%–12%) (Fig. 2c). This suggested the abundance of added PG showed no significant difference of BEP efficiency.

The incubation time, however, showed evident changes in BEP efficiency. The BEP efficiency significantly increased from 15.75% (6dPG + ANG treatment) to 30.84% (10dPG + ANG treatment). Finally, it was elevated to 37.81% for the 15dPG + ANG treatment (Fig. 2d). Without *A. niger*, the P dissolution efficiencies maintained at 10%, i.e., 9% for 6dPG treatment, 11% for 10dPG treatment, and 12% for the 15dPG treatment (Fig. 2d). The role of *A. niger* in the process of P dissolution in PG was significant.

Functional groups analysis of ATR-IR

In the ATR-IR spectra (Fig. 3), the absorption band at 596 cm^{-1} was characteristic of phosphate P-O vibrational modes[46]. This peak displayed maximal intensity in MPG and HPG treatments (Fig. 3). The absorption band at 780 cm^{-1} was attributed to P-O vibration based on

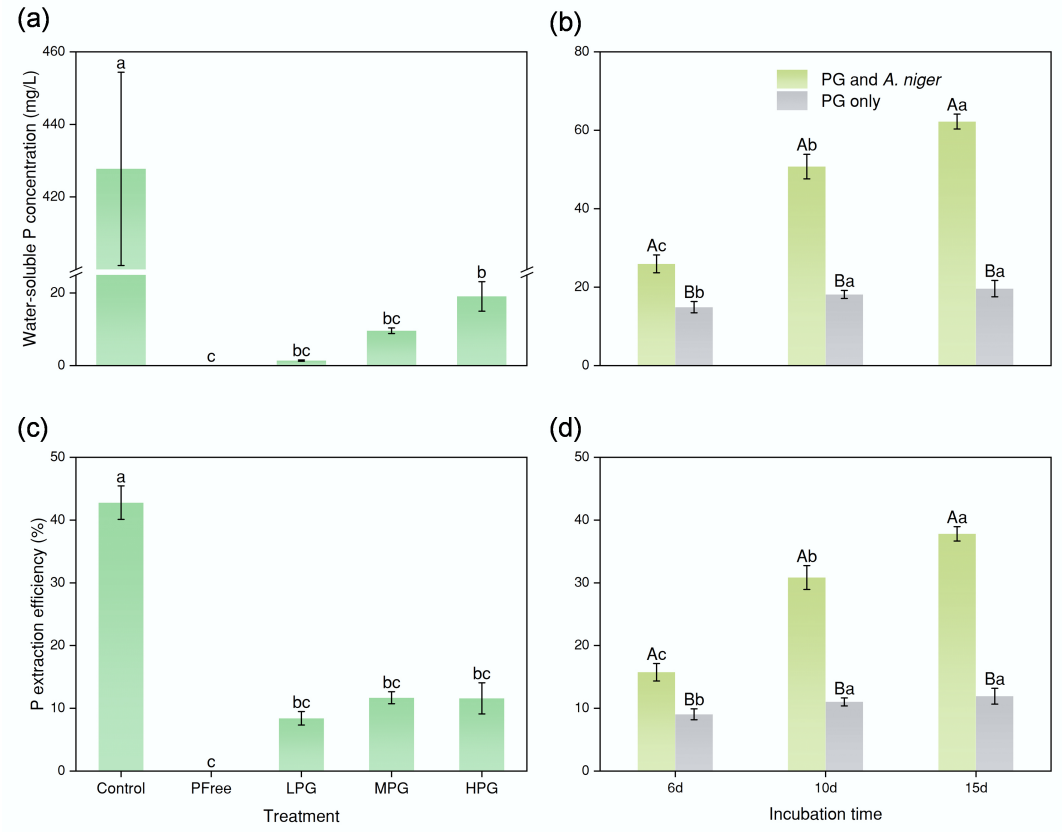

Fig. 2 Effect of bioextraction of P. (**a**) and (**c**) concentrations of water-soluble P and P bioextraction efficiency by *A. niger* after six days of incubation. (**b**) and (**d**) concentrations of water-soluble P and P extraction efficiency after six, 10, and 15 d of incubation, respectively (the P involved in the figure pertained solely to P presented in the solution, excluding P in fungal pellets). In (**a**) and (**c**), the lowercase letter labels indicate significant differences among different treatments. If two treatments had the same lowercase letter, there was no significant difference; otherwise, there was a considerable difference. In (**b**) and (**d**), the capital letter labels indicate whether there was a substantial difference between the treatments PG only or PG and *A. niger* at the same incubation time. The lowercase letters indicate significant differences among incubation times within each treatment (PG only or PG and *A. niger*). The method for determining substantial differences was consistent with the above.

https://doi.org/10.48130/ebp-0025-0018

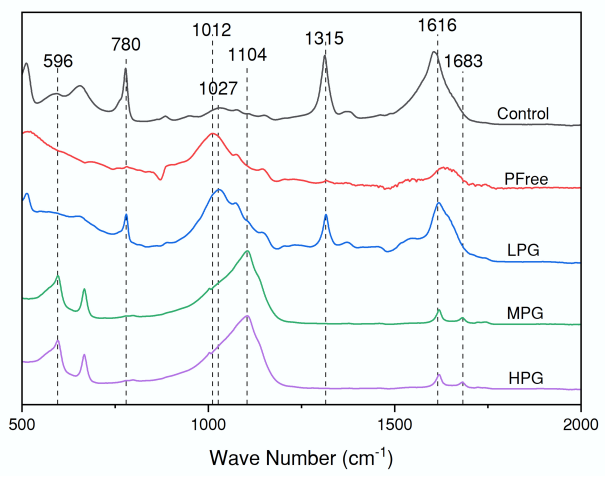

Fig. 3 ATR-IR spectra of the filtered solid phase after incubation for six days.

HPO_4^{2-}. This peak was prominent in both Control and LPG treatments (but with higher intensity in the Control treatment) (Fig. 3). The absorption band at 1,012 cm^{-1} was assigned to C–O and C–C vibrations from microbial polysaccharides[47,48], which was prominent in PFree treatment (Fig. 3). The 1,027 cm^{-1} band represented ν1 and ν3 P-O vibration of PO_4^{3-} (Fig. 3)[49,50]. Compared with the Control treatment, the intensity of this peak was significantly enhanced in the LPG treatments (Fig. 3). At 1,104 cm^{-1}, the spectrum exhibited a mixed vibrational mode resulting from the combination of P-O (for PO_4^{3-}) and S-O (for SO_4^{2-})[51]. The intensity distribution of this peak was similar to that of the 596 cm^{-1} peak (Fig. 3). As the mass of PG increased, there was more SO_4^{2-} in the system, and the intensity of this peak got stronger (Fig. 3). The absorption band at 1,315 cm^{-1} represented symmetric stretching vibrations of C-O from $C_2O_4^{2-}$ while that at 1,616 cm^{-1} represented the asymmetric stretching vibrations from $HC_2O_4^-$[52]. Both peaks were characteristic of oxalic acid (Fig. 3). The 1,683 cm^{-1} peak represented the C=O stretching vibration (Fig. 3)[53]. The intensity of the three peaks above in the spectra of Control and LPG treatments was higher than that in MPG and HPG treatments (Fig. 3). When the mass of PG reached 0.5 g, the peaks of oxalic acid functional groups were masked by the peak of S-O vibration in PG (Fig. 3).

NanoSIMS, SEM-EDS, and GWB analysis

Signals from the CN element in the NanoSIMS images were used to locate areas of biological composition (Fig. 4a, d). The signal of the P element further highlighted the cellular structure of *A. niger* (Fig. 4b, e), which was highly coincident with that of the CN element. P maps indicated that most of the P in PG was within *A. niger* cells for fungus growth during incubation (Fig. 4b, e)[44]. Meanwhile, enrichment of the P element was observed in specific *A. niger* cells (Fig. 4b, e), indicating cell division. In addition, the signal of the S element displayed the basal sulfur distribution, which can mainly be ascribed to sulfur-containing proteins. S maps indicated that the abundant SO_4^{2-} in PG could be absorbed by *A. niger* for the synthesis of cellular proteins (Fig. 4e, f).

The contents of Ca and Fe in the PG were 32.19 and 0.49 wt%, respectively, based on XRF analysis. The solid phases obtained from LPG, MPG, and HPG treatments were observed by SEM (Fig. 5). SEM image and EDS result confirmed the formation of CaC_2O_4, which was tightly interacted by hyphae of *A. niger* (Fig. 5a). During incubation, oxalic acid secreted by *A. niger* interacted with the $CaSO_4$ adsorbed by its hyphae (Fig. 5b). Then, the $C_2O_4^{2-}$ ionized from oxalic acid replaced the SO_4^{2-} in $CaSO_4$, resulting in the formation of CaC_2O_4 (Fig. 5a). Meanwhile, as the P in PG slowly dissolved into the solution, Fe in the solution was mineralized to strengite (Fig. 5c, d).

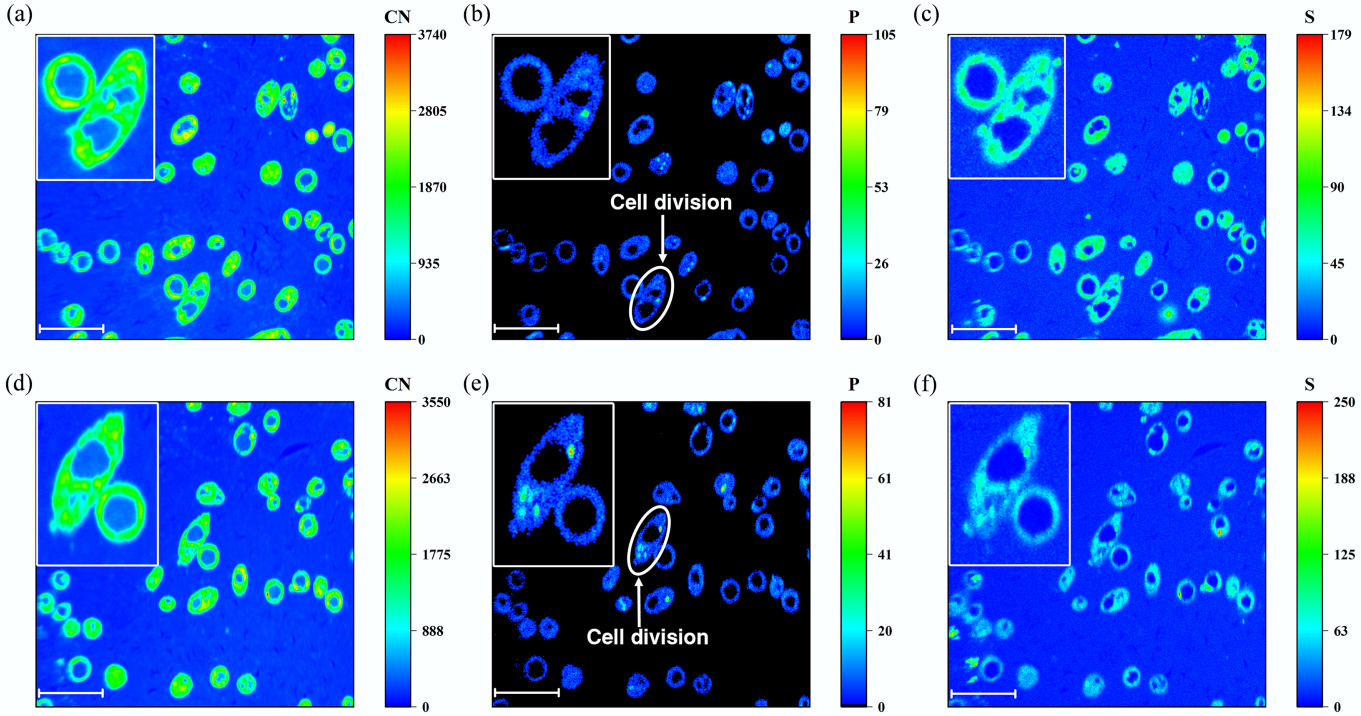

Fig. 4 NanoSIMS images of High PG treatment after 6 days of incubation. (**a**) and (**d**) CN element distribution. (**b**) and (**e**) P element distribution. (**c**) and (**f**) S element distribution. (**a**)–(**c**) were from the same region, while figures (**d**)–(**f**) were from another region. The scale bar of all the figures was 10 μm.

GWB simulation revealed that with the increase of pH, PO_4^{3-} tended to combine with Ca^{2+} and then mineralized into hydroxylapatite (Fig. 6b). Meanwhile, the abundance of Ca^{2+} and $C_2O_4^{2-}$ in the solution induced substantial precipitation of CaC_2O_4 (Fig. 6).

Discussion

The residual P in PG is the portion that remained unextracted during sulfuric acid leaching. This makes re-extraction of P usually difficult and of low-efficiency. The secretion of oxalic acid has been reported to promote P release from insoluble phosphates with high efficiency. The BEP efficiency in this study confirmed that biogenic oxalic acid is fully capable of dissolving the residual P within PG (see Fig. 2). Moreover, as a typical filamentous fungi, *A. niger* can capture and wrap dispersed PG particles in the medium through its hyphal network during the incubation process (see Fig. 5b)[54]. Then, fungal hyphae can extend the distribution of oxalic acid on PG particles[55]. These two pathways together would provide a favorable microenvironment for PG dissolution. In agriculture, the hyphal network of *A. niger* can extend into various soil micropores and regions inaccessible to plant root systems, thereby expanding the scope of P solubilization in the soil system[56,57].

The BEP efficiency of PG by *A. niger* reached as high as ~40% for the 15dPG + ANG treatment (see Fig. 2d), which was comparable to its BEP efficiency from pure $Ca_3(PO_4)_2$ (see Fig. 2c). This result was attributed to the sustainability provided by *A. niger* during the BEP process. In addition, the extraction efficiency of PG could be further improved by extending the incubation time of *A. niger*. A portion of the extracted P in solution was utilized for the growth of *A. niger* and participated in biological metabolic processes (see Fig. 4b, e)[56]. Microorganisms require P uptake for the synthesis of essential biomolecules such as ATP and cell wall phospholipids[40, 58]. The release of P from PG promised the fungal metabolism. Meanwhile, the fungal metabolism ensured the sustainability of the BEP process[59]. Moreover, the P in the biomass of these fungal cells can be easily applied as fertilizer or in the biochemical industry[60].

Traditional chemical extraction methods (e.g., sulfuric acid leaching) indiscriminately dissolve more Ca, Fe, Si, and other minor elements than BEP[61]. However, dissolved Ca tends to recombine with P and re-mineralize into hydroxylapatite (see Fig. 6b). Similarly, Fe^{3+} demonstrates a distinct propensity to mineralize with PO_4^{3-} into strengite (see Figs 5c, d, and 6). Both mineralization pathways would significantly reduce the efficiency of P extraction. The dissolution of Si results in the formation of silica gel, which physically hinders contact between sulfuric acid and PG, thereby indirectly impairing P extraction efficiency[62,63]. This can explain why chemical P extraction methods inevitably retain ~1% residual P in PG globally. Conversely, BEP exhibits highly selective P recovery, particularly at low P concentrations. Additionally, the microorganisms specifically target P while minimizing the co-solubility of impurities[64].

The release of P from PG and the metabolism of *A. niger* may have formed a positive feedback loop. Primarily, the acidity of PG would create a favorable environment for the incubation of *A. niger*. With the PG addition, the biomass and bioactivity of *A. niger* were enhanced (see Fig. 1a). Then, *A. niger* would continuously secrete oxalic acid during incubation. The H^+ ionized from oxalic acid provided a more favorable microenvironment for P dissolution. Meanwhile, $C_2O_4^{2-}$ mineralized with Ca^{2+} to form CaC_2O_4, thereby reducing the reabsorption of dissolved P by free Ca^{2+} [42]. Subsequently, the solubilization of P would be enhanced. In addition, the

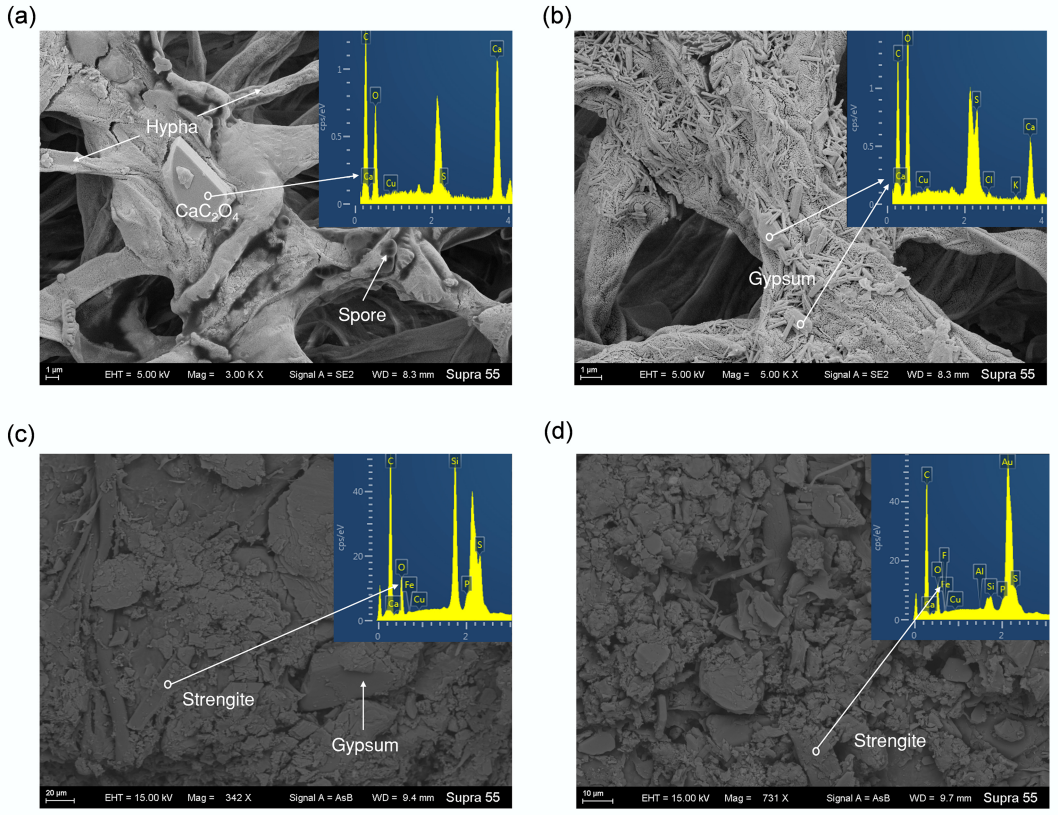

Fig. 5 SEM and EDS images of minerals formed during incubation. (**a**) Calcium oxalate from Low PG treatment. (**b**) Gypsum particles adsorbed by *A. niger* hyphae from High PG treatment. (**c**) and (**d**) Strengite from Moderate PG treatment.

https://doi.org/10.48130/ebp-0025-0018

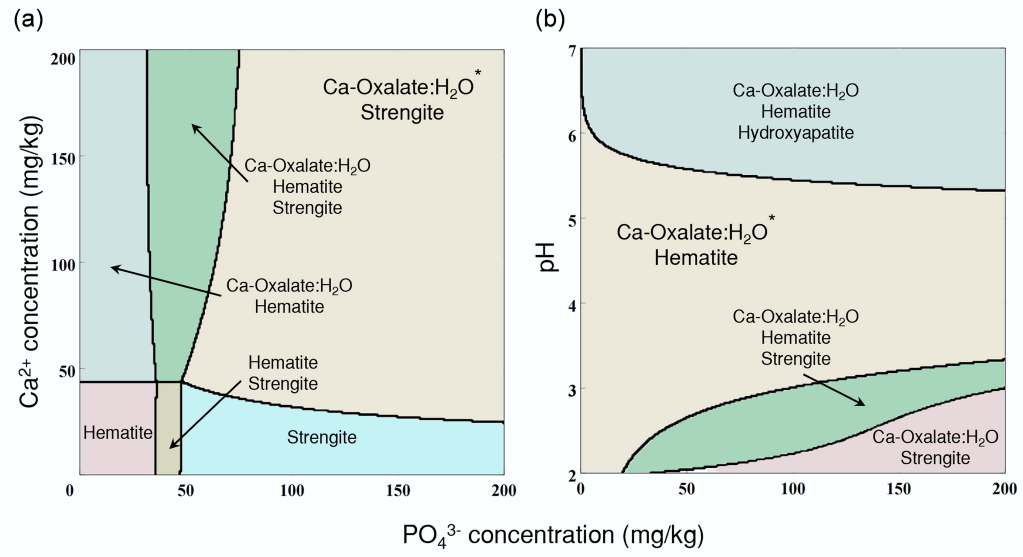

Fig. 6 Simulation of the *A. niger*-phosphogypsum interaction system. (**a**) Geochemical simulated mineralization under different concentrations of PO_4^{3-} and Ca^{2+} by the GWB Act2 module. (**b**) Geochemical simulated mineralization under different concentrations of PO_4^{3-}, and different pH by the GWB Act2 module.

released P would be absorbed by *A. niger* cells to meet their nutritional requirements (see Fig. 4e)[58]. The abundant SO_4^{2-} in PG would maintain the positive feedback loop of the BEP process. SO_4^{2-} was absorbed by *A. niger* through the sulfate transporter, then reduced to SO_3^{2-} or S^{2-} via the sulfate assimilation pathway, ultimately synthesizing into sulfur-containing amino acids such as cysteine[32]. PG also contained other nutrients required by microorganisms, such as K (0.8%) and Mg (0.3%), which may be essential during incubation[65]. Such a positive feedback loop would ensure the sustainability of fungal growth and the BEP process.

After bioextraction, the P in the solution existed as PO_4^{3-}, which is available to plants. Although the P content in PG is relatively low, it is readily soluble due to prior acidulation with sulfuric acid. For plants, the main issue is the low utilization rate of P[54,66]. The biosystem composed of *A. niger* and PG can be utilized for the production of highly efficient microbial phosphate fertilizers. The hyphae of *A. niger* can build a bridge between available P and the plant root system, thereby maximizing the utilization efficiency of P[23]. When such a biosystem is applied to the soil, plants will absorb the P released by the fungal hyphae through their root systems[67]. Meanwhile, the plant roots and fungi will also form a positive feedback regulation. The plant root system secretes organic matters (such as phosphatases and amino acid derivatives) to stimulate *A. niger* to grow more vigorously[68], thereby secreting more organic acids to release insoluble P[69].

Conclusions

The presence of PSF *A. niger* significantly increased the release efficiency of P from PG. The efficiency of BEP increased with increasing incubation time. There might be a positive feedback loop between the incubation of *A. niger* and the recovery of P from PG. BEP of *A. niger* provides a broad prospect for the treatment of substantial PG waste and the improvement of the shortage of soil available P in agricultural fields.

Author contributions

The authors confirm their contributions to the paper as follows: Zhenyu Chao: investigation, methodology, validation, writing – original draft, writing – review and editing; Haoxuan Li: writing – original draft, writing – review and editing; Jiakai Ji: writing – original draft, writing – review and editing; Xin Sun: investigation, data curation; Yuhang Sun: investigation, data curation; Meiyue Xu: investigation, data curation; Ying Wang: investigation, data curation; Da Tian: supervision, project administration; Haoming Chen: supervision, project administration; Dan Yu: supervision, project administration; Zhen Li: conceptualization, funding acquisition, writing – review and editing. All authors reviewed the results and approved the final version of the manuscript.

Data availability

The datasets generated during the current study are available from the corresponding author on reasonable request.

Funding

This work was supported by the National Key R&D Program of China (Grant No. 2023YFC3707600), and the Research Fund Program of Guangdong Provincial Key Laboratory of Environmental Pollution Control and Remediation Technology (Grant No. 2023B1212060016).

Declarations

Competing interests

The authors declare that they have no known competing financial interests or personal relationships that could have appeared to influence the work reported in this paper.

Author details

[1]College of Resources and Environmental Sciences, Nanjing Agricultural University, Nanjing, Jiangsu 210095, China; [2]Anhui Province Key

Lab of Farmland Ecological Conservation and Pollution Prevention, College of Resources and Environment, Anhui Agricultural University, Hefei 230036, China; [3]School of Environmental and Biological Engineering, Nanjing University of Science and Technology, Nanjing 210094, China; [4]North China Power Engineering Co., Ltd of China Power Engineering Consulting Group, Beijing 100120, China; [5]Jiangsu Provincial Key Lab of Organic Solid Waste Utilization, Nanjing Agricultural University, Nanjing 210095, China; [6]Jiangsu Provincial Key Laboratory of Coastal Saline Soil Resources Utilization and Ecological Conservation, Nanjing 210095, China

References

[1] Wei Z, Deng Z. 2022. Research hotspots and trends of comprehensive utilization of phosphogypsum: bibliometric analysis. *Journal of Environmental Radioactivity* 242:106778

[2] Qin X, Cao Y, Guan H, Hu Q, Liu Z, et al. 2023. Resource utilization and development of phosphogypsum-based materials in civil engineering. *Journal of Cleaner Production* 387:135858

[3] Bouargane B, Laaboubi K, Biyoune MG, Bakiz B, Atbir A. 2023. Effective and innovative procedures to use phosphogypsum waste in different application domains: review of the environmental, economic challenges and life cycle assessment. *Journal of Material Cycles and Waste Management* 25:1288–1308

[4] Fuleihan NF. 2012. Phosphogypsum disposal-the pros & cons of wet versus dry stacking. *Procedia Engineering* 46:195–205

[5] Chernysh Y, Yakhnenko O, Chubur V, Roubik H. 2021. Phosphogypsum recycling: a review of environmental issues, current trends, and prospects. *Applied Sciences* 11:1575

[6] Bilal E, Bellefqih H, Bourgier V, Mazouz H, Dumitraş DG, et al. 2023. Phosphogypsum circular economy considerations: a critical review from more than 65 storage sites worldwide. *Journal of Cleaner Production* 414:137561

[7] Huang L, Liu Y, Ferreira JFS, Wang M, Na J, et al. 2022. Long-term combined effects of tillage and rice cultivation with phosphogypsum or farmyard manure on the concentration of salts, minerals, and heavy metals of saline-sodic paddy fields in Northeast China. *Soil and Tillage Research* 215:105222

[8] Palencia P, Luis Guerrero J, Millán R, Mosqueda F, Pedro Bolívar J. 2024. Utilization of phosphogypsum and red mud in alfalfa cultivation. *Heliyon* 10:e28751

[9] Lambers H, Barrow NJ. 2020. P_2O_5, K_2O, CaO, MgO, and basic cations: pervasive use of references to molecules that do not exist in soil. *Plant and Soil* 452:1–4

[10] Qi H, Ma B, Tan H, Su Y, Lu W, et al. 2022. Influence of fluoride ion on the performance of PCE in hemihydrate gypsum pastes. *Journal of Building Engineering* 46:103582

[11] Oliveira V, Labrincha J, Dias-Ferreira C. 2018. Extraction of phosphorus and struvite production from the anaerobically digested organic fraction of municipal solid waste. *Journal of Environmental Chemical Engineering* 6:2837–2845

[12] Cordell D, Brownlie WJ, Esham M. 2021. Commentary: time to take responsibility on phosphorus: towards circular food systems. *Global Environmental Change* 71:102406

[13] Sharma RK, Adholeya A, Puri A, Das M. 2012. Bioextraction: the interface of biotechnology and green chemistry. In *Biomass Conversion: The Interface of Biotechnology, Chemistry and Materials Science*, eds Baskar C, Baskar S, Dhillon RS. Berlin, Heidelberg: Springer. pp. 435–457 doi: 10.1007/978-3-642-28418-2_14

[14] Johnson DB. 2014. Biomining—biotechnologies for extracting and recovering metals from ores and waste materials. *Current Opinion in Biotechnology* 30:24–31

[15] Pilon-Smits EAH, Freeman JL. 2006. Environmental cleanup using plants: biotechnological advances and ecological considerations. *Frontiers in Ecology and the Environment* 4:203–210

[16] Monachon M, Albelda-Berenguer M, Lombardo T, Cornet E, Moll-Dau F, et al. 2021. Evaluation of an alternative biotreatment for the extraction of harmful iron and sulfur species from waterlogged wood. *The European Physical Journal Plus* 136:937

[17] Ristović I, Štyriaková D, Štyriaková I, Šuba J, Širadović E. 2022. Bioleaching process for copper extraction from waste in alkaline and acid medium. *Minerals* 12:100

[18] Vardanyan A, Zhang R, Khachatryan A, Melkonyan Z, Hovhannisyan A, et al. 2024. Extraction of copper from copper concentrate by indigenous association of iron-oxidizing bacteria. *Separations* 11:124

[19] Wang X, Ma L, Wu J, Xiao Y, Tao J, et al. 2020. Effective bioleaching of low-grade copper ores: insights from microbial cross experiments. *Bioresource Technology* 308:123273

[20] Martín-Hernández E, Taifouris M, Martín M. 2022. Addressing the contribution of agricultural systems to the phosphorus pollution challenge: a multi-dimensional perspective. *Frontiers in Chemical Engineering* 4:970707

[21] Feng J, Chen L, Xia T, Ruan Y, Sun X, et al. 2023. Microbial fertilizer regulates C:N:P stoichiometry and alleviates phosphorus limitation in flue-cured tobacco planting soil. *Scientific Reports* 13:10276

[22] Peng F, He W, Gu R, Liang D, Li D, et al. 2024. Enhancing phosphorus release and recovery from waste activated sludge by citric acid treatment and cyclic extraction. *Chemical Engineering Journal* 501:157461

[23] García-Berumen JA, Flores de la Torre JA, de los Santos-Villalobos S, Espinoza-Canales A, Echavarría-Cháirez FG, et al. 2025. Phosphorus dynamics and sustainable agriculture: the role of microbial solubilization and innovations in nutrient management. *Current Research in Microbial Sciences* 8:100326

[24] Sharma SB, Sayyed RZ, Trivedi MH, Gobi TA. 2013. Phosphate solubilizing microbes: sustainable approach for managing phosphorus deficiency in agricultural soils. *SpringerPlus* 2:587

[25] Alori ET, Glick BR, Babalola OO. 2017. Microbial phosphorus solubilization and its potential for use in sustainable agriculture. *Frontiers in Microbiology* 8:971

[26] Tian L, Han M, Liang K, Liu H, Feng B. 2024. Profiling of farmland microorganisms in maize and minor-grain crops under extreme drought conditions. *Applied Soil Ecology* 204:105743

[27] Zheng Y, Yu S, Li Y, Peng J, Yu J, et al. 2022. Efficient bioimmobilization of cadmium contamination in phosphate mining wastelands by the phosphate solubilizing fungus *Penicillium oxalicum* ZP6. *Biochemical Engineering Journal* 187:108667

[28] Coreño-Alonso J, Coreño-Alonso O, Martínez-Rosales JM. 2014. Apatite formation on alumina: the role of the initial adsorption of calcium and phosphate ions. *Ceramics International* 40:4909–4915

[29] Beheshti M, Alikhani HA, Pourbabaee AA, Etesami H, Asadi Rahmani H, et al. 2022. Enriching periphyton with phosphate-solubilizing microorganisms improves the growth and concentration of phosphorus and micronutrients of rice plant in calcareous paddy soil. *Rhizosphere* 24:100590

[30] Bolo P, Kihara J, Mucheru-Muna M, Njeru EM, Kinyua M, et al. 2021. Application of residue, inorganic fertilizer and lime affect phosphorus solubilizing microorganisms and microbial biomass under different tillage and cropping systems in a Ferralsol. *Geoderma* 390:114962

[31] Rawat P, Das S, Shankhdhar D, Shankhdhar SC. 2021. Phosphate-solubilizing microorganisms: mechanism and their role in phosphate solubilization and uptake. *Journal of Soil Science and Plant Nutrition* 21:49–68

[32] Fu A, Li Q, Li Y, Chen Y, Wei Y, et al. 2025. Nidustrin A, cysteine-retained emestrin with a unique 18-membered macrocyclic lactone from the endophytic fungus *Aspergillus nidulans*. *Bioorganic Chemistry* 155:108105

[33] Zhang X, Rajendran A, Grimm S, Sun X, Lin H, et al. 2023. Screening of calcium- and iron-targeted phosphorus solubilizing fungi for agriculture production. *Rhizosphere* 26:100689

[34] Li Y, Xu Z, Zhang L, Chen W, Feng G. 2024. Dynamics between soil fixation of fertilizer phosphorus and biological phosphorus mobilization determine the phosphorus budgets in agroecosystems. *Agriculture, Ecosystems & Environment* 375:109174

[35] Timofeeva A, Galyamova M, Sedykh S. 2022. Prospects for using phosphate-solubilizing microorganisms as natural fertilizers in agriculture. *Plants* 11:2119

https://doi.org/10.48130/ebp-0025-0018

[36] da Silva LI, Pereira MC, Xavier de Carvalho AM, Buttros VH, Pasqual M, et al. 2023. Phosphorus-solubilizing microorganisms: a key to sustainable agriculture. *Agriculture* 13:432
[37] Dusengemungu L, Kasali G, Gwanama C, Mubemba B. 2021. Overview of fungal bioleaching of metals. *Environmental Advances* 5:100083
[38] Duan H, Zhang X, Zhao X, Xu C, Zhang D, et al. 2025. Study on biogenic acid-mediated enhanced leaching of lepidolite by *Aspergillus niger* based on transcriptomics. *Bioresource Technology* 418:131920
[39] Ashrafi-Saiedlou S, Rasouli-Sadaghiani M, Samadi A, Barin M, Sepehr E. 2024. *Aspergillus niger* as an eco-friendly agent for potassium release from K- bearing minerals: isolation, screening and culture medium optimization using Plackett-Burman design and response surface methodology. *Heliyon* 10:e29117
[40] Yu L, Wang T, Wang B, Pan L. 2024. The mechanism of short hypha formation and high protein production system mediated by cell wall integrity signaling pathway in *Aspergillus niger*. *International Journal of Biological Macromolecules* 283:137413
[41] Priha O, Sarlin T, Blomberg P, Wendling L, Makinen J, et al. 2014. Bioleaching phosphorus from fluorapatites with acidophilic bacteria. *Hydrometallurgy* 150:269–275
[42] de Oliveira Mendes G, de Freitas ALM, Pereira OL, da Silva IR, Bojkov Vassilev N, et al. 2014. Mechanisms of phosphate solubilization by fungal isolates when exposed to different P sources. *Annals of Microbiology* 64:239–249
[43] Chaerun SK, Sulistyo RS, Minwal WP, Mubarok MZ. 2017. Indirect bioleaching of low-grade nickel limonite and saprolite ores using fungal metabolic organic acids generated by *Aspergillus niger*. *Hydrometallurgy* 174:29–37
[44] Qiu J, Song X, Li S, Zhu B, Chen Y, et al. 2021. Experimental and modeling studies of competitive Pb (II) and Cd (II) bioaccumulation by *Aspergillus niger*. *Applied Microbiology and Biotechnology* 105:6477–6488
[45] Meng L, Pan S, Zhou L, Santasup C, Su M, et al. 2022. Evaluating the survival of *Aspergillus niger* in a highly polluted red soil with addition of Phosphogypsum and bioorganic fertilizer. *Environmental Science and Pollution Research* 29:76446–76455
[46] Chen H, Zhang J, Tang L, Su M, Tian D, et al. 2019. Enhanced Pb immobilization via the combination of biochar and phosphate solubilizing bacteria. *Environment International* 127:395–401
[47] Gómez-Ordóñez E, Rupérez P. 2011. FTIR-ATR spectroscopy as a tool for polysaccharide identification in edible brown and red seaweeds. *Food Hydrocolloids* 25:1514–1520
[48] Pereira L, Amado AM, Critchley AT, van de Velde F, Ribeiro-Claro PJA. 2009. Identification of selected seaweed polysaccharides (phycocolloids) by vibrational spectroscopy (FTIR-ATR and FT-Raman). *Food Hydrocolloids* 23:1903–1909
[49] Kourkoumelis N, Lani A, Tzaphlidou M. 2012. Infrared spectroscopic assessment of the inflammation-mediated osteoporosis (IMO) model applied to rabbit bone. *Journal of Biological Physics* 38:623–635
[50] Garip S, Severcan F. 2010. Determination of simvastatin-induced changes in bone composition and structure by Fourier transform infrared spectroscopy in rat animal model. *Journal of Pharmaceutical and Biomedical Analysis* 52:580–588
[51] Chen S, Chen J, He X, Su Y, Jin Z, et al. 2023. Comparative analysis of colloid-mechanical microenvironments on the efficient purification of phosphogypsum. *Construction and Building Materials* 392:132037
[52] Yeasmin S, Singh B, Kookana RS, Farrell M, Sparks DL, et al. 2014. Influence of mineral characteristics on the retention of low molecular weight organic compounds: a batch sorption-desorption and ATR-FTIR study. *Journal of Colloid and Interface Science* 432:246–257
[53] Guo Q, Yi H, Jia F, Song S. 2022. Design of MoS_2/MMT bi-layered aerogels integrated with phase change materials for sustained and efficient solar desalination. *Desalination* 541:116028
[54] Ölmez F, Mustafa Z, Türkölmez Ş, Bildirici AE, Ali SA, et al. 2024. Phosphate-solubilizing fungus (PSF) - mediated phosphorous solubilization and validation through Artificial intelligence computation. *World Journal of Microbiology and Biotechnology* 40:376
[55] Li SL, Xu S, Wang TJ, Yue FJ, Peng T, et al. 2020. Effects of agricultural activities coupled with karst structures on riverine biogeochemical cycles and environmental quality in the karst region. *Agriculture, Ecosystems & Environment* 303:107120
[56] Kumar A, Teja ES, Mathur V, Kumari R. 2020. Phosphate-solubilizing fungi: current perspective, mechanisms and potential agricultural applications. In *Agriculturally Important Fungi for Sustainable Agriculture*, eds Yadav A, Mishra S, Kour D, Yadav N, Kumar A. Cham: Springer. pp. 121–141 doi: 10.1007/978-3-030-45971-0_6
[57] Zhang L, Zhou J, George TS, Limpens E, Feng G. 2022. Arbuscular mycorrhizal fungi conducting the hyphosphere bacterial orchestra. *Trends in Plant Science* 27:402–411
[58] Duhamel S. 2025. The microbial phosphorus cycle in aquatic ecosystems. *Nature Reviews Microbiology* 23:239–255
[59] Gurav PP, Kollah B, Shirale AO, Yadav DK, Mohanty SR, et al. 2024. Phosphorus solubilizing microorganisms: a technique for enhancing phosphorus use efficiency. *Journal of Plant Nutrition* 47:3906–3920
[60] Luyckx L, Sousa Correia DS, Van Caneghem J. 2021. Linking phosphorus extraction from different types of biomass incineration ash to ash mineralogy, ash composition and chemical characteristics of various types of extraction liquids. *Waste and Biomass Valorization* 12:5235–5248
[61] Wang M, Yuan X, Dong W, Fu Q, Ao X, et al. 2023. Gradient removal of Si and P impurities from phosphogypsum and preparation of anhydrous calcium sulfate. *Journal of Environmental Chemical Engineering* 11:110312
[62] Rivera RM, Ulenaers B, Ounoughene G, Binnemans K, Van Gerven T. 2018. Extraction of rare earths from bauxite residue (red mud) by dry digestion followed by water leaching. *Minerals Engineering* 119:82–92
[63] Cheng S, Li W, Vaughan J, Ma X, Chan J, et al. 2025. Advances in the integrated recovery of valuable components from titanium-bearing blast furnace slag: a review. *Sustainable Materials and Technologies* 44:e01384
[64] Brucker E, Kernchen S, Spohn M. 2020. Release of phosphorus and silicon from minerals by soil microorganisms depends on the availability of organic carbon. *Soil Biology and Biochemistry* 143:107737
[65] Soumare A, Sarr D, Diédhiou AG. 2023. Potassium sources, microorganisms and plant nutrition: challenges and future research directions. *Pedosphere* 33:105–115
[66] Khan MS, Zaidi A, Ahemad M, Oves M, Wani PA. 2010. Plant growth promotion by phosphate solubilizing fungi – current perspective. *Archives of Agronomy and Soil Science* 56:73–98
[67] Zhang L, Deng X, Xiao J, Zhao W, Zou P, et al. 2025. Root metabolites regulated by FERONIA promote phosphorus-solubilizing rhizobacteria enrichment induced by *Arabidopsis thaliana* coping with phosphorus deficiency. *Microbiological Research* 292:128030
[68] Khourchi S, Elhaissoufi W, Loum M, Ibnyasser A, Haddine M, et al. 2022. Phosphate solubilizing bacteria can significantly contribute to enhance P availability from polyphosphates and their use efficiency in wheat. *Microbiological Research* 262:127094
[69] Rolfe SA, Griffiths J, Ton J. 2019. Crying out for help with root exudates: adaptive mechanisms by which stressed plants assemble health-promoting soil microbiomes. *Current Opinion in Microbiology* 49:73–82